

Composed material models for nonlinear behavior of reinforced concrete

Tayfun Dede^{*1} and Yusuf Ayvaz^{2a}

¹Department of Civil Engineering, Karadeniz Technical University, Trabzon, Türkiye

²Department of Civil Engineering, Yıldız Technical University, Istanbul, Türkiye

(Received April 25, 2012, Revised March 5, 2013, Accepted March 31, 2013)

Abstract. The purpose of this study is to present different composed material models for reinforced concrete structures (RC). For this aim a nonlinear finite element analysis program is coded in MATLAB. This program contains several yield criteria and stress-strain relationships for compression and tension behavior of concrete. In this study, the well-known criteria, Drucker-Prager, von Mises, Mohr Coulomb, Tresca, and two new criteria, Hsieh-Ting-Chen and Bresler-Pister, are taken into account. It is concluded that the coded program, the new yield criteria, and the models considered can be effectively used in the nonlinear analysis of reinforced concrete beams.

Keywords: composed material model; elastic behavior; plastic behavior; nonlinear analysis

1. Introduction

It is generally not possible to obtain the non-linear response and the failure behavior of concrete by using conventional linear procedures since concrete material has a complex behavior under monotonic or cyclic loading. In order to predict the behavior of reinforced concrete structures more reliable, several studies have been made in the field of nonlinear analysis of RC structures. Köksal *et al.* (2009) made a practical approach for modeling FRP wrapped concrete columns by using Drucker-Prager criterion. Wang and Hsu (2001) applied the nonlinear finite element analysis to different types of RC structures using a new set of constitutive models. Bratina *et al.* (2004) presented a study on materially and geometrically nonlinear analysis of RC planar frames by dealing with the fiber-based constitutive equations of concrete and steel. Zhao *et al.* (2004) studied the load-deflection and failure characteristics of deep RC coupling beams. Pankaj and Lin (2005) used two similar continuum plasticity material models to examine the influence of the material modeling on the seismic response of RC frame structures. Belmouden and Lestuzzi (2007) investigated the post peak modeling and nonlinear performance of RC structural walls. Bischoff (2001), Bischoff (2003), Stramandinoli and Rovere (2008), and Dede and Ayvaz (2009) studied on RC structures by using tension stiffening effect. Barros and Martins (2012) presented a

*Corresponding author, Ph.D., E-mail: tayfundede@gmail.com

^aPh.D., E-mail: yayvaz@yildiz.edu.tr

study on nonlinear analysis of service stresses in Reinforced Concrete sections-closed form solutions. Mahini and Ronagh (2011) made a numerical model for monitoring the hysteretic behaviour of CFRP-retrofitted RC exterior beam-column joints.

Constitutive models proposed for RC can be classified into orthotropic models, nonlinear elastic models, plasticity models, endochronic models, fracture mechanics models and micromodels (Ayoub and Flippou 1998). Among these models, plasticity models, which frequently used because of its simple and direct representation of multiaxial stress (Park and Kim 2005), need a yield function, a hardening rule, a flow rule and a stress-strain relationship to construct the plastic material matrix for the plastic behavior of concrete.

A review of the literature indicates that there are not any studies based on the Bresler-Pister and Hsieh-Ting-Chen criteria for the plastic behavior of concrete. This yield function can be found in the books concerning with the plasticity theory, but its plasticity material matrix or any application of this function to the RC structures is not found.

In this paper, derivation of plastic material matrix based on Bresler-Pister and Hsieh-Ting-Chen yield function and the applications of these functions to the RC beams are presented. For this aim, a nonlinear finite element analysis program is coded in MATLAB. This program contains several yield criteria and stress-strain relationships for the compression and tension behavior of concrete. In the nonlinear analysis, the well-known criteria, Drucker-prager, von Mises, Tresca and Mohr Coulomb and new criteria, Bresler-Pister and Hsieh-Ting-Chen are taken into account. The elastic-perfectly plastic and Saenz stress-strain relationships in compression behavior of concrete and tension stiffening in tension behavior of concrete are used with four different yield criteria mentioned above.

2. Composed material matrix for RC

The material matrix of a reinforced concrete finite element is constructed to be the sum of the material matrices of the concrete and reinforcement. In this calculation, the reinforcement embedded in the concrete elements is represented by an equivalent element. The material matrices of reinforced concrete element are given, respectively, as

$$[D] = [D_c] + [D_s] = \frac{E}{1-\nu^2} \begin{bmatrix} 1 & \nu & 0 \\ \nu & 1 & 0 \\ 0 & 0 & (1-\nu)/2 \end{bmatrix} + \begin{bmatrix} P_x E_s & 0 & 0 \\ 0 & \rho_y E_s & 0 \\ 0 & 0 & 0 \end{bmatrix} \quad (1)$$

where D_c and D_s are the material matrices of concrete and equivalent reinforcement elements, respectively. E_s is the modulus of elasticity of reinforcement, ρ_x and ρ_y are the reinforcement ratios in global directions of the x and y axes, respectively.

3. Constitutive modeling of concrete

In this section, the derivation of material stiffness matrix of reinforced concrete is presented for plane stress problem.

3.1 Yield criteria for concrete

The concrete is assumed to be elastic until it reaches the yield limit. Beyond yielding, plastic deformations take place. So, plastic deformations remain after removing the loading. The well-known criteria, Drucker-Prager, von Mises, Mohr Coulomb and Tresca, and new criteria, Bresler-Pister and Hsieh-Ting-Chen are used to construct the plastic material stiffness matrix for concrete material.

The well-known yield functions for Drucker Prager, von Mises, Mohr Coulomb and Tresca are given by the following equations, respectively (Chen 1982).

$$f = \alpha I_1 + \sqrt{J_2} - k \quad (2)$$

$$f = \sqrt{J_2} - k \quad (3)$$

$$f = I_1 \sin \phi + \frac{1}{2} \left[3(1 - \sin \phi) \sin \theta + \sqrt{3}(3 + \sin \theta) \cos \theta \right] \sqrt{J_2} - 3 \cos \phi \quad (4)$$

$$f = 4J_2^3 - 27J_3^2 - 36k^2J_2^2 + 96k^4J_2 - 64k^6 \quad (5)$$

where α and k are the material parameters, c is cohesion, ϕ is the internal friction angle, I_1 is the first invariant of stress tensor, J_2 is the second invariant of deviator stress tensor, J_3 is the third invariant of deviator stress tensor, and θ is the angle of similarity, and $\cos(3\theta)$ is given by the following equation.

$$\cos(3\theta) = \frac{3\sqrt{3}}{2} \frac{J_3}{J_2^{3/2}} \quad (6)$$

The Bresler-Pister criterion (Bresler and Pister 1958) is the extension of Drucker Prager criterion. This yield function in terms of octahedral stresses is given by Eq. (7). The failure envelope and π -plane of Bresler-Pister criterion are given in Fig. 1.

$$\frac{\tau_{oct}}{f'_c} = a - b \left(\frac{\sigma_{oct}}{f'_c} \right) + c \left(\frac{\sigma_{oct}}{f'_c} \right)^2 \quad (7)$$

where a , b , and c are the material parameters of this yield criterion, f'_c is the uniaxial compressive cylinder strength, σ_{oct} is the octahedral normal stress and τ_{oct} is the octahedral shear stress. The octahedral normal and shear stresses are given by the following equations, respectively.

$$\begin{aligned} \tau_{oct} &= \sqrt{\frac{2}{3}} J_2 \\ \sigma_{oct} &= \frac{I_1}{3} \end{aligned} \quad (8)$$

Substituting Eq. (8) into Eq. (7) and rewriting Eq. (7), the Bresler-Pister yield criterion in terms of stress invariant can be obtained, and it is given as

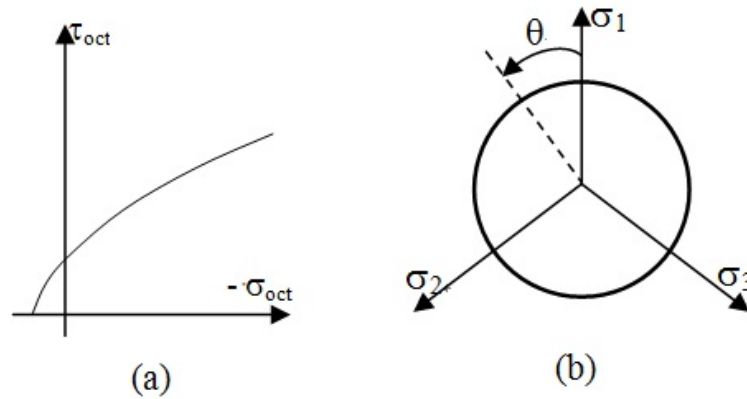


Fig. 1 (a) Failure envelope and (b) π - Plane of Bresler-Pister criterion

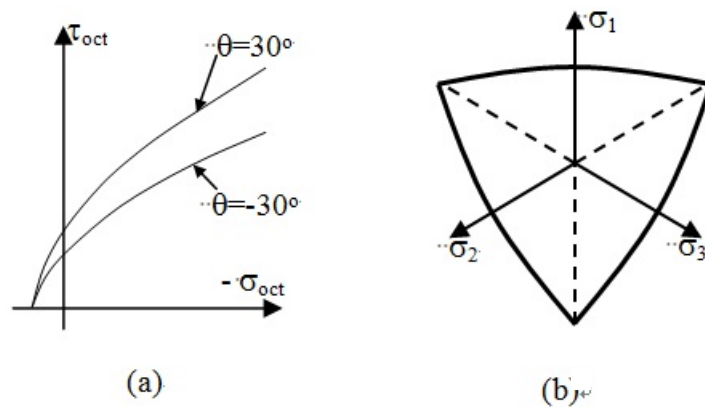


Fig. 2 (a) Failure envelope and (b) π - Plane of Hsieh-Ting-Chen criterion

$$f = \left(\frac{c}{9f_c'^2}\right)I_1^2 - \left(\frac{b}{3f_c'}\right)I_1 - \left(\frac{\sqrt{2}}{\sqrt{3}f_c'}\right)\sqrt{J_2} - a. \tag{9}$$

The Hsieh-Ting-Chen criterion (Hsieh *et al.* 1979) is given by Eq. (10). Failure envelope and π -plane of Hsieh-Ting-Chen criterion are given in Fig. 2.

$$f = \sqrt{2J_2} - \frac{1}{2a} \left[-(b \cos \theta + c) + \sqrt{(b \cos \theta + c)^2 - 4a \left(\sqrt{3}d \frac{I_1}{3} - 1 \right)} \right] \tag{10}$$

where $a, b, c,$ and d are the material parameters of this yield criterion.

3.2 Elastic and plastic parts of material matrix for RC material

In the plasticity theory, the total strain can be assumed to be the sum of the elastic strain and plastic strain as given by Eq. (11), and stress increment, $d\sigma_{ij}$, for strain increment, $d\varepsilon_{ij}$, is given by Eq. (12) (Chen 1984).

$$d\varepsilon_{ij} = d\varepsilon_{ij}^e + d\varepsilon_{ij}^p \quad (11)$$

$$d\sigma_{ij} = D_{ijkl}^{ep} d\varepsilon_{ij} \quad (12)$$

where D_{ijkl} is the elastic-plastic material matrix. In the case of associated flow rule the general form of this matrix is given as

$$D_{ijkl}^{ep} = D_{ijkl} + D_{ijkl}^p \quad (13)$$

where D_{ijkl}^{ep} is the elastic material matrix. The plastic material matrix is calculated as

$$D_{ijkl}^p = -\frac{D_{ijkl} \frac{\partial f}{\partial \sigma_{ij}} \frac{\partial f}{\partial \sigma_{pq}} D_{pqkl}}{h + \frac{\partial f}{\partial \sigma_{ij}} D_{ijkl} \frac{\partial f}{\partial \sigma_{kl}}} \quad (14)$$

where

$$h = \phi H^p \frac{\partial f}{\partial \tau} \quad (15)$$

where

$$\phi = \frac{1}{\tau} \frac{\partial f}{\partial \sigma_{ij}} \sigma_{ij} \quad (16)$$

where τ is von Mises effective stress $\tau = \sqrt{3J_2}$ and H^p is the slope of uniaxial stress-strain curve.

The gradient $\frac{\partial f}{\partial \sigma_{ij}}$ can be written as

$$\frac{\partial f}{\partial \sigma_{ij}} = \frac{\partial f}{\partial I_1} \frac{\partial I_1}{\partial \sigma_{ij}} + \frac{\partial f}{\partial J_2} \frac{\partial J_2}{\partial \sigma_{ij}} + \frac{\partial f}{\partial J_3} \frac{\partial J_3}{\partial \sigma_{ij}} \quad (17)$$

where

$$\frac{\partial J_3}{\partial \sigma_{ij}} = t_{ij}, t_{ij} = s_{ik} s_{kj} - \frac{2}{3} J_2 s_{ij} \quad i = j = k = 1, 2, 3 \quad (18)$$

By taking the derivatives of Eq. (9) with respect to I_1 , J_2 and J_3 , the following equations can be obtained for Bresler-Pister yield criterion.

$$\begin{aligned}\frac{\partial f}{\partial I_1} &= \frac{2c}{9f_c^2} I_1 - \frac{b}{3f_c'} \\ \frac{\partial f}{\partial J_2} &= -\frac{1}{\sqrt{6J_2} f_c'} \\ \frac{\partial f}{\partial J_3} &= 0\end{aligned}\quad (19)$$

Similar derivatives of Eq. (9) with respect to I_1 , J_2 and J_3 yield the following equations for Hsieh-Ting-Chen yield criterion.

$$\begin{aligned}\frac{\partial f}{\partial I_1} &= \frac{\sqrt{3}}{3h_2} d \\ \frac{\partial f}{\partial J_2} &= \frac{1}{\sqrt{2J_2}} - \frac{b \sin \theta}{2a} \left[1 - \frac{b \cos \theta + c}{h_2} \right] \frac{\partial \theta}{\partial J_2} \\ \frac{\partial f}{\partial J_3} &= -\frac{b \sin \theta}{2a} \left[1 - \frac{b \cos \theta + c}{h_2} \right] \frac{\partial \theta}{\partial J_3}\end{aligned}\quad (20)$$

where

$$\begin{aligned}h_2 &= \sqrt{(b \cos \theta + c)^2 - 4a \left(\sqrt{3}d \frac{I_1}{3} - 1 \right)} \\ \frac{\partial \theta}{\partial J_2} &= \frac{3\sqrt{3J_3}}{4} \frac{1}{J_2^{5/2}} \frac{1}{\sin 3\theta} \\ \frac{\partial \theta}{\partial J_3} &= \frac{\sqrt{3}}{2} \frac{1}{J_2^{3/2}} \frac{1}{\sin 3\theta}\end{aligned}\quad (21)$$

The gradient $\frac{\partial I_1}{\partial \sigma_{ij}}$ and $\frac{\partial J_2}{\partial \sigma_{ij}}$ are called to be the kronecker delta and deviatoric stress tensor, respectively, and they are given in Eqs. (22) and (23), respectively.

$$\frac{\partial I_1}{\partial \sigma_{ij}} = \delta_{ij} = \begin{bmatrix} 1 & 0 & 0 \\ 0 & 1 & 0 \\ 0 & 0 & 1 \end{bmatrix}\quad (22)$$

$$\frac{\partial J_2}{\partial \sigma_{ij}} = s_{ij} = \sigma_{ij} - \frac{I_1}{3} \delta_{ij}\quad (23)$$

By substituting Eq. (19), Eq. (22) and Eq. (23) into Eq. (17), the following equation can be obtained for Bresler-Pister criterion.

$$\frac{\partial f}{\partial \sigma_{ij}} = \left(\frac{2c}{9f_c'^2} I_1 - \frac{b}{3f_c'} \right) \delta_{ij} - \left(\frac{1}{\sqrt{6J_2} f_c} \right) \quad (24)$$

By substituting Eq. (18), Eq. (20), Eqs. (22) and (23) into Eq. (17), the following equation can be obtained for Hsieh-Ting-Chen criterion.

$$\begin{aligned} \frac{\partial f}{\partial \sigma_{ij}} = & \left(-\frac{\sqrt{3}}{3h_2} d \right) \delta_{ij} \\ & + \left(\frac{1}{\sqrt{2J_2}} - \frac{b \sin \theta}{2a} \left[1 - \frac{b \cos \theta + c}{h_2} \right] \right) \frac{\partial \theta}{\partial J_2} s_{ij} \\ & - \frac{b \sin \theta}{2a} \left[1 - \frac{b \cos \theta + c}{h_2} \right] \frac{\partial \theta}{\partial J_3} t_{ij} \end{aligned} \quad (25)$$

The gradient $\frac{\partial f}{\partial \tau}$ given in Eq. (14) can be obtained based on Bresler-Pister and Hsieh-Ting-Chen criteria, and they are given in Eqs. (26) and Eq. (27), respectively.

$$\frac{\partial f}{\partial \tau} = \frac{-\sqrt{2}}{3f_c'} \quad (26)$$

$$\frac{\partial f}{\partial \tau} = \frac{\sqrt{2}}{\sqrt{3}} + \frac{b}{2a} \frac{\partial \cos \theta}{\partial \tau} \left[1 - \frac{b \cos \theta + c}{h_2} \right] \quad (27)$$

where

$$\frac{\partial \cos \theta}{\partial \tau} = -2 \frac{\partial \theta}{\partial J_2} \sqrt{\frac{J_2}{3}} \sin \theta \quad (28)$$

4. Stress-strain curves for concrete

In order to define stress-strain relationship for concrete, several stress-strain curves are proposed by researchers (Wang and Hsu 2001, Hognestad 1951, Popovics 1973, Collins and Porasz 1989, Saenz 1964, Hoshikuma *et al.* 1996, Park and Paulay 1975, Desayi and Krishnan 1964, Bentz 1999, Izumo *et al.* 1992). The Saenz (1964) and elastic-perfectly plastic stress-strain

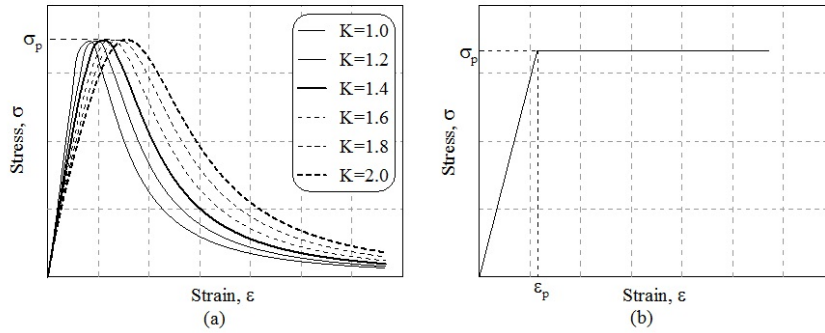


Fig. 3 Stress-strain curve of (a) Saenz and (b) elastic-perfectly plastic model for concrete under compression

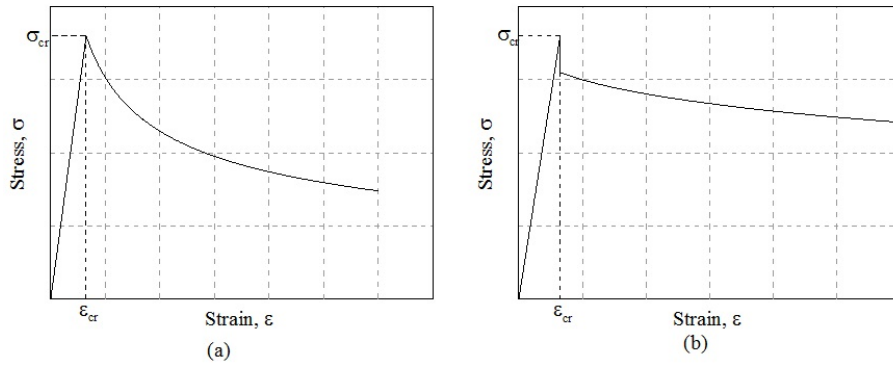


Fig. 4 Stress-strain curve of (a) Wang and Hsu (2001) and (b) Vecchio 1982 model for concrete under tension

relationships used for the behavior of concrete in compression are given in Eq. (29) and in Eq. (30), respectively, and they are illustrated in Fig. 3.

$$\sigma_c = \sigma_p \frac{K \left(\frac{\epsilon_c}{\epsilon_p} \right) - \left(\frac{\epsilon_c}{\epsilon_p} \right)^2}{1 + A \left(\frac{\epsilon_c}{\epsilon_p} \right) + B \left(\frac{\epsilon_c}{\epsilon_p} \right)^2 + C \left(\frac{\epsilon_c}{\epsilon_p} \right)^3} \tag{29}$$

$$\begin{aligned} \sigma_c &= - \left(\frac{\epsilon_c}{\epsilon_p} \right) \sigma_p && \text{if } \epsilon_p < \epsilon_c < 0 \\ \sigma_c &= -\sigma_p && \text{if } \epsilon_p < \epsilon_c < 0 \end{aligned} \tag{30}$$

where

$$A = C + K - 2; B = 1 - 2C; C = K \frac{K_\sigma - 1}{(K_\varepsilon - 1)^2} - \frac{1}{K_\varepsilon} \quad (31)$$

$$K = E \frac{\varepsilon_p}{\sigma_p}; K_\varepsilon = \frac{\varepsilon_f}{\varepsilon_p}; K_\sigma = \frac{\sigma_p}{\sigma_f}$$

where ε_f and σ_f are the control point coordinates on descending branch of stress-strain curve, σ_c is the concrete compressive stress, ε_c is the concrete compressive strain, σ_p is the peak concrete compressive stress, ε_p is the concrete compressive strain corresponding to σ_p , and E is the modulus of elasticity of concrete.

The stress-strain curve of concrete in tension proposed by Wang and Hsu (2001) is shown in Fig. 4(a). The ascending and descending branches of this curve are given by the following equation.

$$\begin{aligned} \sigma_t &= E\varepsilon_t & \text{if } \varepsilon_t \leq 0 \\ \sigma_t &= \sigma_{cr} \left(\frac{\varepsilon_{cr}}{\varepsilon_t} \right)^{0.4} & \varepsilon_t > \varepsilon_{cr} \end{aligned} \quad (32)$$

where σ_t is the concrete tensile stress, ε_t is the concrete tensile strain, σ_{cr} is the concrete cracking stress, and ε_{cr} is the concrete cracking strain.

The other stress-strain curve of concrete in tension used in this paper is Vecchio 1982 curve. This curve is shown in Fig. 4(b) and its stress-strain relationship (Wong 1992) is given by the following equation.

$$\begin{aligned} \sigma_t &= E\varepsilon_t & \text{if } \varepsilon_t \leq \varepsilon_{cr} \\ \sigma_t &= \frac{\sigma_{cr}}{1 + \sqrt{200\varepsilon_t}} & 0 < \varepsilon_{cr} < \varepsilon_t \end{aligned} \quad (33)$$

5. Numerical examples

The applicability and verification of the developed program are demonstrated by comparing the results obtained in this study with the experimental and analytical results of different RC beams: Bresler-Scordelis beam, J4 beam and Shear Panel Beam.

5.1 Bresler-Scordelis beam

The first RC member used to validate the program coded is Bresler-Scordelis beam. It is simply supported RC beam (Wang and Hsu 2001, Bresler and Scordelis 1964) and is shown in Fig. 5. The longitudinal reinforcement consists of 4 steel bars with the total area of 2580 mm². The concrete has a compressive strength of 24.5 MPa and elastic modulus of 21300 MPa. The elastic modulus of reinforcement is 191400 MPa.

In the finite element modeling, 4-noded rectangular plane-stress element is used. This element

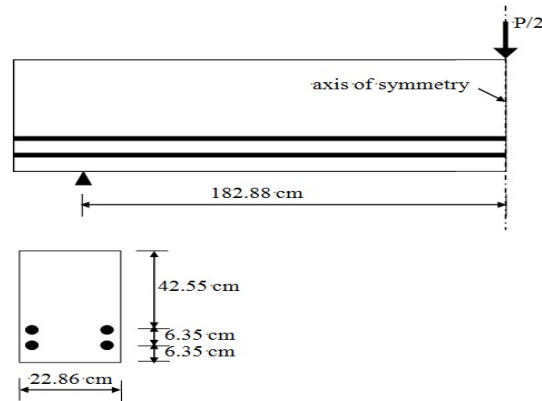


Fig. 5 Geometry and cross-section of bresler-scordelis beam

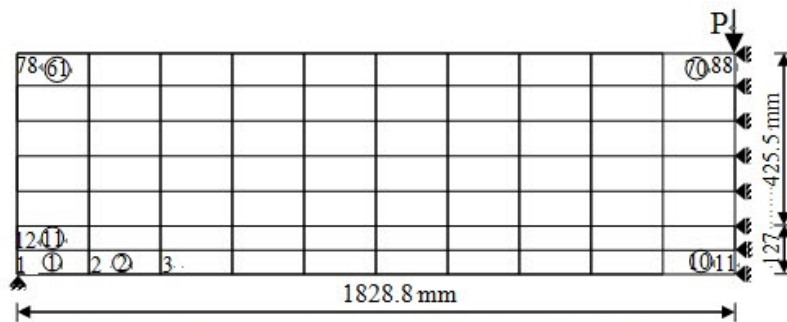


Fig. 6 Finite element modeling of bresler-scordelis beam

has two displacement degrees of freedom at a point and 8 displacement degrees of freedom in an element. Perfect bond between concrete and reinforcement is assumed.

Since the method used herein is a numerical method, the finite element method, there is always some error in the results, depending on the mesh size used to solve the problem. Therefore, for the sake of accuracy in the results, rather than starting with a finite element mesh size, the mesh size to produce the desired accuracy is determined. To find out the required mesh size, convergence of the maximum displacement is checked for different mesh sizes. In conclusion, the results have an acceptable error when using approximately 70 elements. Therefore, 70 elements which is also the number of the elements used in the literature are used in this study in order to compare the results obtained in this study with the experimental and theoretical results given in the literature. Finite element modeling of this beam is given in Fig. 6.

The results of the nonlinear analysis of this beam by using different yield criteria with two different tension stress-strain curves (Wang and Hsu 2001, Vecchio 1982) for the tension behavior of concrete and with two different compression stress-strain curves (elastic-perfectly plastic and Saenz) for the compression behavior of concrete are given in Fig. 7. These results are compared with each other and with the experimental result taken from the literature (Wang and Hsu 2001). As seen from this figure, the load-displacement curves obtained in this study are in good agreement with the experimental result.

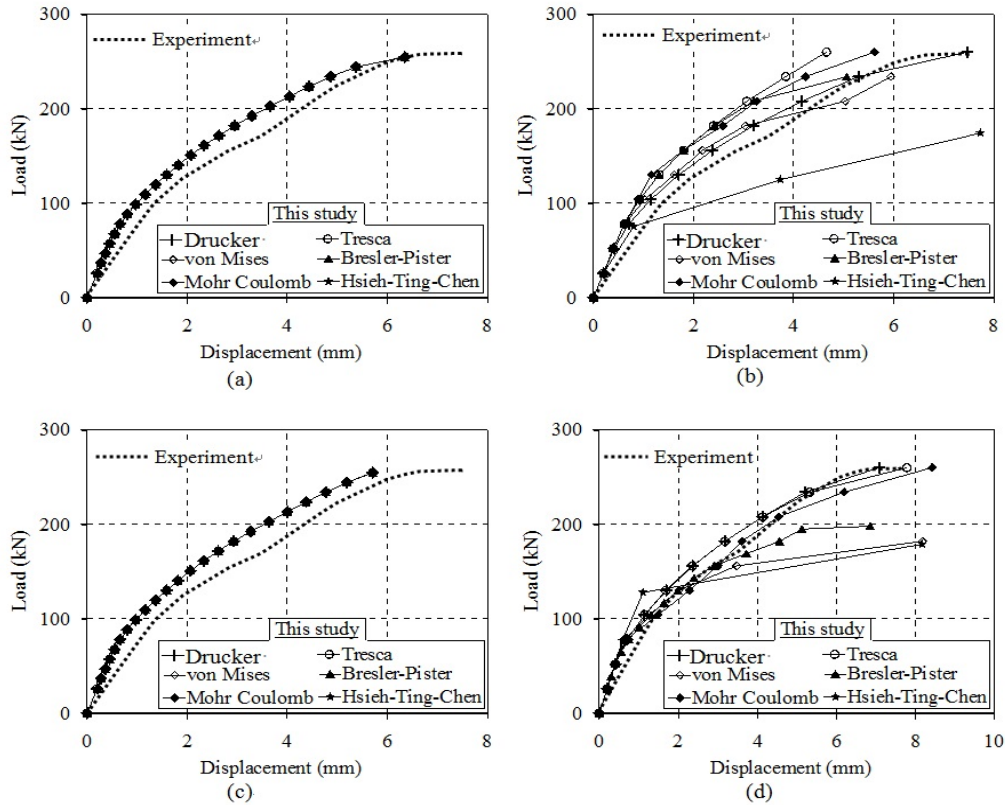


Fig. 7 Load-displacement curves of Bresler-Scordelis beam based on different yield criteria (a) for Wang and Hsu (2001) in tension and elastic-perfectly plastic in compression, (b) for Wang and Hsu (2001) in tension and Saenz in compression, (c) for Vecchio 1982 in tension and elastic-perfectly plastic in compression and (d) for Vecchio 1982 in tension and Saenz in compression behavior of concrete.

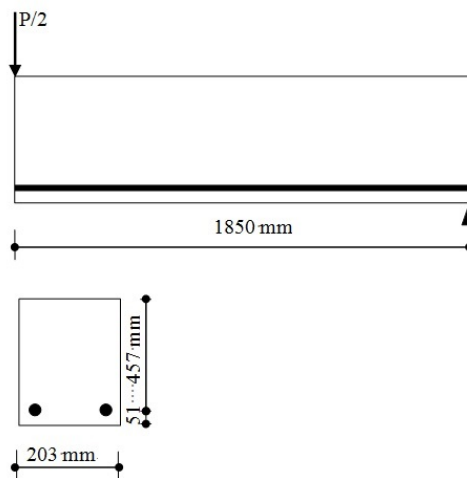


Fig. 8 Geometry and cross-section of J4 beam

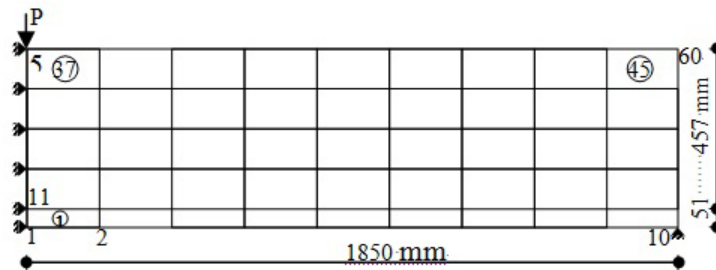


Fig. 9 Finite element modeling of J4 beam

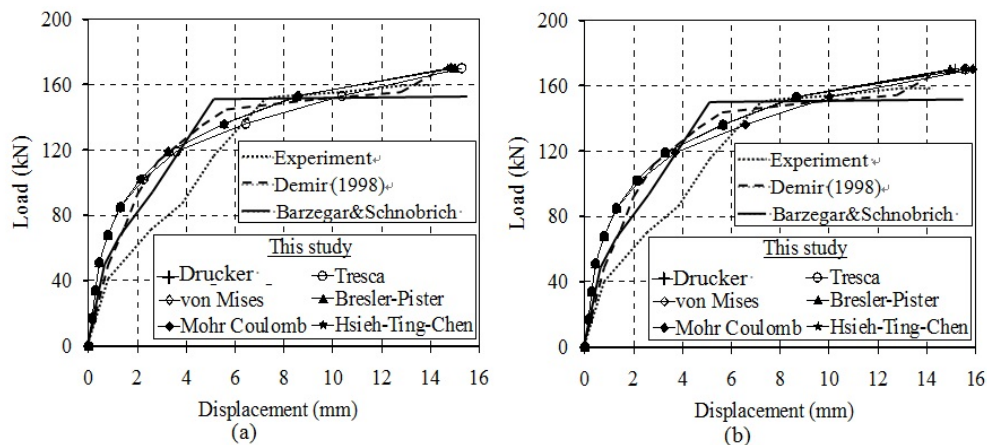


Fig. 10 Load-displacement curves of J4 beam based on different yield criteria (a) for Wang and Hsu (2001) in tension and elastic-perfectly plastic in compression, (b) for Vecchio 1982 in tension and Saenz in compression behavior of concrete.

5.2 Simply supported J4 beam

The second RC member used to validate the program coded is J4 beam. It is simply supported (Demir 1998, Burns and Siess 1962) and is shown in Fig. 8. The longitudinal reinforcement consists of 2 steel bars with total area of 1021 mm^2 . The concrete has a compressive strength of 33 MPa and elastic modulus of 26200 MPa. The elastic modulus of reinforcement is 203000 MPa.

The finite element mesh convergence of this beam is also studied. It is concluded that the results have an acceptable error when using approximately 45 elements. This element number is also the number of the elements used in the literature. Therefore, using this element number makes the comparison of the results obtained in this study with the experimental and theoretical results given in the literature possible. Finite element modeling of this beam is given in Fig. 9.

The results of the nonlinear analysis of this beam by using different yield criteria with two different tension stress-strain curves (Wang and Hsu 2001, Vecchio 1982) for the tension behavior of concrete and with two different compression stress-strain curves (elastic-perfectly plastic and Saenz) for the compression behavior of concrete are given in Fig. 10. These results are compared

with each other and with the experimental (Burns and Siess 1962) and analytical results (Demir 1998, Barzegar and Schnobrich 1962). As seen from this figure, the load-displacement curves obtained in this study are in good agreement with the experimental and analytical results. Also, the results of new criteria, Bresler-Pister and Hsieh-Ting-Chen, show good agreement with the results obtained by using the other criteria and with the experimental and analytical results.

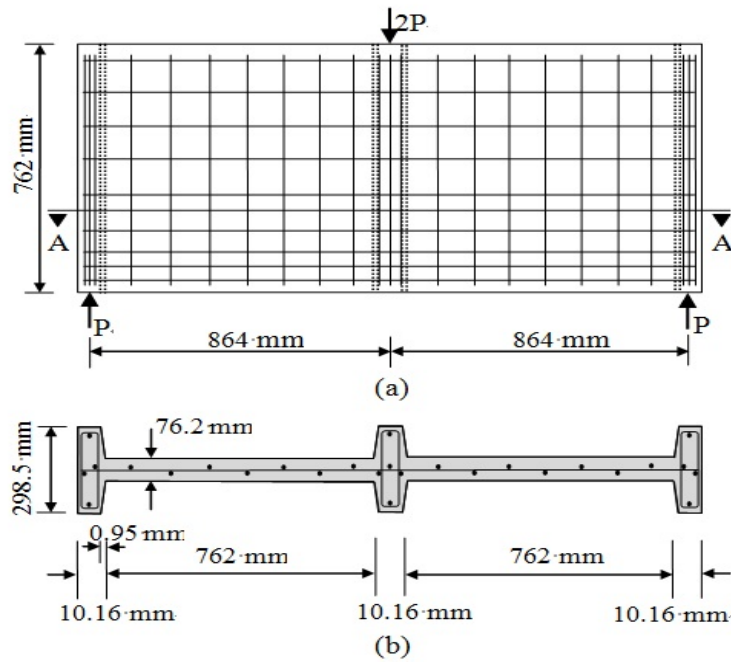


Fig. 11 Geometry and cross-section of shear panel beam

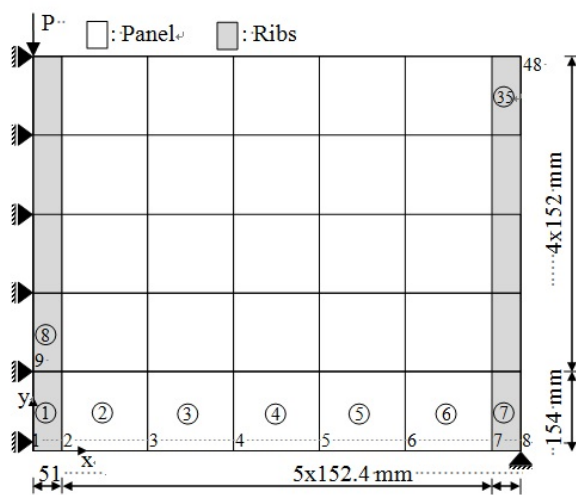


Fig. 12 Finite element modeling of panel beam

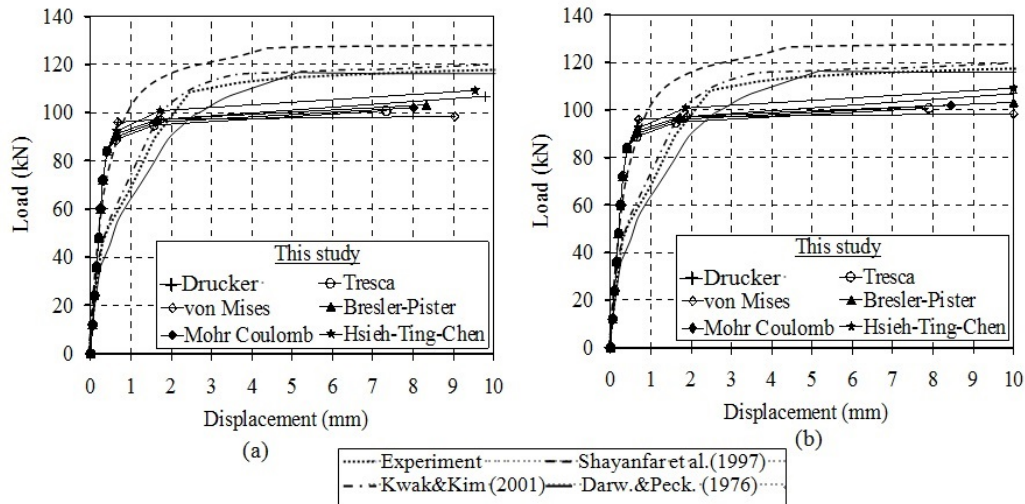


Fig. 13 Load-displacement curves of shear panel beam based on different yield criteria for (a) Wang and Hsu (2001) in tension and elastic-perfectly plastic in compression, (b) Vecchio 1982 in tension and Saenz in compression behavior of concrete.

Table 1 Reinforcement ratios

Elements	Reinforcement ratio		
	Direction	Panel	Ribs
1-7	x	0.0092	0.0023
	y	0.0092	0.0047
8-35	x	0.0183	0.0047
	y	0.0092	0.0047

5.3 RC shear panel beam

The third RC member used to validate the program coded is shear panel beam. It is used by many researchers and is shown in Fig. 11. The reinforcement ratios of this structure are given in Table 1. The concrete has a compressive strength of 26.8 MPa and elastic modulus of 20,000 MPa. The elastic modulus of reinforcement is 190,000 MPa.

The finite element mesh convergence of this beam is also studied. It is concluded that the results have an acceptable error when using approximately 35 elements. This element number is also the number of the elements used in the literature. Therefore, using this element number makes the comparison of the results obtained in this study with the experimental and theoretical results given in the literature possible. Because of the symmetry in geometry and loading, half part of this beam is modeled and finite element modeling of half part of this beam is given in Fig. 12.

The results of the nonlinear analysis of this beam by using different yield criteria with two different tension stress-strain curves (Wang and Hsu 2001, Vecchio 1982) for the tension behavior of concrete and with two different compression stress-strain curves (elastic-perfectly plastic and Saenz) for the compression behavior of concrete are given in Fig. 13. These results are compared with each other and with the experimental (Cervenka and Gerstle 1971) and analytical results

(Shayanfar *et al.* 1997, Darwin and Pecknold 1976, Kwak and Kim 2001).

As seen from this figure, the load-displacement curves obtained in this study are in good agreement with the experimental and analytical results. Also, the results of new criteria, Bresler-Pister and Hsieh-Ting-Chen, show excellent agreement with the results obtained by using the other criteria and with the experimental and analytical results.

6. Conclusions

Analytical models are presented for the nonlinear behavior of reinforced concrete structures. Based on the Bresler-Pister and Hsieh-Ting-Chen yield functions, plastic material matrices for concrete material are constructed. Also, different stress-strain curves of concrete for tension and compression behavior are taken into account and the well-known criteria, Drucker-Prager, von Mises, Tresca and Mohr Coulomb are also used for the plastic behavior of concrete.

The computer program coded in this study is useful for predicting the behavior of reinforced concrete structures. This program contains the well-known criteria (Drucker-prager, von Mises, Tresca and Mohr Coulomb), new criteria (Bresler-Pister and Hsieh-Ting-Chen), stress-strain curves for the compression behavior of concrete (elastic-perfectly plastic and Saenz model), and tension stiffening model (Wang and Hsu 2001, Vecchio 1982 model).

The proposed models, Bresler-Pister and Hsieh-Ting-Chen criteria can be effectively used in the nonlinear analysis of reinforced concrete beams.

References

- Ayoub, A. and Filippou, F.C. (1998), "Nonlinear finite-element analysis of RC shear panels and wall", *J. Struct. Eng.*, **124**(3), 298-308.
- Barros, H.F.M. and Martins, R.A.F. (2012), "Nonlinear analysis of service stresses in reinforced Concrete sections-closed form solutions", *Comput. Concr.*, **10**(5), 541-555.
- Barzegar, F. and Schnobrich, W.C. (1962), "Nonlinear Finite Element Analysis of RC Under Short Term Monotonic Loading", 0, SRS No.530, University of Illinois, Urbana.
- Belmouden, Y. and Lestuzzi, P. (2007) "Analytical model for predicting nonlinear reversed cyclic behavior of reinforced concrete structural walls", *Eng. Struct.*, **29**(7), 1263-1276.
- Bentz, E.C. (1999) "Sectional analysis of reinforced concrete members", Ph.D. Thesis, University of Tronto.
- Bitchoff, P.H. (2003), "Tension stiffening and cracking of steel fiber-reinforced concrete", *J. Mat. Civil Eng.*, **15**(2), 174-182.
- Bitchoff, P.H. (2001), "Effects of shrinkage on tension stiffening and cracking in reinforced concrete", *Can. J. Civil Eng.*, **28**(3), 363-374.
- Bratina, S., Saje, M. and Planinc, I. (2004), "On materially and geometrically nonlinear analysis of reinforced concrete planar frames", *Int. J. Solids Struct.*, **41**(24-25), 7181-7207.
- Bresler, B. and Pister, K.S. (1958), "Strenght of concrete under combined stresses", *J. Am. Concr. Inst.* **55**(9), 321-345.
- Bresler, B. and Scordelis, A.C. (1964), "Shear strength of reinforced concrete beams-series II", SESM Report No 64-2, University of California, Berkeley.
- Burns, N.H. and Siess, C.P. (1962), "Load-deformations characteristics of beam-column connections in reinforced concrete", Civil Engineering Studies, SRS No.243, University of Illinois, Urbana.
- Cervenka, V. and Gerstle, K.H. (1971), "Inelastic analysis of reinforced concrete panels. Part I: theory", *Assoc Bridge Struct. Engrs. Publs*, **31**(11), 31-45.

- Chen, W.F. (1982), *Plasticity in Reinforced Concrete*, McGraw-Hill, New York.
- Chen, W.F. (1994), *Constitutive Equation for Engineering Materials*, Elsevier, New York.
- Collins, M.P. and Porasz, A. (1989), "Shear design of high strength concrete", *CEB Bulletin d' Information*, **193**, 77-83.
- Darwin, D. and Pecknold, D.A. (1976), "Analysis of RC shear panels under cyclic loading", *J. Struct. Div. ASCE*, **102**(2), 355-69.
- Dede, T. and Ayvaz, Y. (2009), "Nonlinear analysis of reinforced concrete beam with/without tension stiffening effect", *Mat. Des.*, **30**(9), 3846-3851.
- Demir, F. (1998), "Applications of finite element in reinforced concrete elements", Ph.D. Thesis, Istanbul Technical University.
- Desayi, P. and Krishnan, S. (1964), "Equation for the stress-strain curve of concrete". *ACI J.* 6, 345-350.
- Hognestad, E. (1951), "A study of combined axial load and lateral load in reinforced concrete members", University of Illinois Engineering Station, Bulletin Series 399:1.
- Hoshikuma, J., Kazuhiko, K., Kazuhiko, N. and Taylor, A.W. (1996), "A model for confinement effect on stress-strain relation of reinforced concrete columns for seismic design", *Proceeding of the 11th World conference Earthquake Engineering*, London.
- Hsieh, S.S., Ting, E.C. and Chen, W.F. (1979), "An Elastic-Fracture Model for Concrete", *Proceeding of the Third Engineering Mechanics Division Specialty Conference*, 437-440.
- Izumo, J., Shin, H., Maekawa, K. and Okamura, H. (1992), "An analytical model for RC panels subjected to in-plane stresses", *Conc. Shear Earth.*, 206-215.
- Köksal, H.O., Doran, B. and Turgay, T. (2009), "A practical approach for modeling FRP wrapped concrete columns", *Const. Buil. Mat.*, **23**(3), 1429-1437.
- Kwak, H.G. and Kim, D.Y. (2001), "Nonlinear analysis of RC shear walls considering tension-stiffening effect", *Comput. Struct.*, **79**(5), 499-517.
- Pankaj, P. and Lin, E. (2005), "Material modeling in the seismic response analysis for the design of RC frames structures", *Eng. Struct.*, **27**(7), 1014-1023.
- Park, H. and Kim, J.Y. (2005), "Plasticity model using multiple failure criteria for concrete in compression", *Int. J. Plast.*, **42**(8), 2303-2322.
- Park, R. and Paulay, T. (1975), *Reinforced concrete structures*, John Wiley & Sons, Inc, United States of America.
- Popovics, S. (1973), "A numerical approach to the complete stress-strain curve of concrete", *Cem. Concr. Res.*, **3**(5), 583-599.
- Ronagh, S.S. and Ronagh, H.R. (2011), "Numerical modelling for monitoring the hysteretic behaviour of CFRP-retrofitted RC exterior beam-column joints", *Struct. Eng. Mech.*, **38**(1), 27-37.
- Saenz, L.P. (1964), "Discussion of equation for the stress-strain curve of concrete by Desayi and Krishnan", *Am. Conc. Ins. J.*, **61**(3), 1229-1235.
- Shayanfar, M.A., Kheyroddin, A. and Mirza, M.S. (1997), "Element size effects in nonlinear analysis of reinforced concrete members", *Comput. Struct.*, **62**(2), 339-352.
- Stramandinoli, R.S.B. and Rovere, H.L.L. (2008), "An efficient tension-stiffening model for nonlinear analysis of reinforced concrete members", *Eng. Struct.*, **30**(7), 2069-2080.
- Wang, T. and Hsu, T.T.C. (2001), "Nonlinear finite element analysis of concrete structures using new Constitutive Models", *Comput. Struct.*, **79**(32), 2781-2791.
- Wong, P.S.L. (1992), "User Facilities for 2D Nonlinear Finite Element Analysis of Reinforced Concrete", M. Sc. Thesis, University of Toronto.
- Zhao, Z.Z., Kwan, A.K.H. and He, X.G. (2004), "Nonlinear finite element analysis of deep reinforced concrete coupling beams", *Eng. Struct.*, **26**(1), 13-25.